

Effect of Thermal Barrier Coating on the performance of the active cooling channel

Siva Karthik C V S S, Santhosh Kumar N, T Kishen Kumar Reddy

Abstract — Actively cooled high speed combustion chamber using hydrocarbon fuel as a coolant, must be designed to cool the liner without exceeding the stoichiometric limit of the fuel required for combustion. Use of high temperature materials such as Nickel and Niobium alloys to sustain the high heat loads, cannot alone achieve the targeted coolant flow rates. Therefore the use of thermal barrier coatings is being investigated by many researchers. In this paper, a comparative performance study was carried out for rectangular and trapezoidal cooling channel configurations using three channel materials viz., Inconel X-750, Nb-Cb-752 and GRCop-84 and three thermal barrier coatings viz., Yittria Stabilized Zirconia (YSZ), La₂Zr₂O₇ and La₂Ce₂O₇. For this purpose a 1-D analytical model was developed in MATLAB for calculating the temperatures and stresses of the active cooling channel. A 2-D numerical simulation was carried out in ANSYS 14.5 to validate the analytical model. Then, using Matlab program the temperatures and stresses were calculated for a range of geometric parameters, in conjunction with various channel materials and TBC materials, for a given set of flow and thermal boundary conditions to bring out the most suitable combination for the application. It was observed that the use of TBCs satisfied the requirement of reduction of the coolant requirements and overall weight per unit area.

Index Terms— Active Cooling Panel, Channel Cross Section, Fins, High Speed Combustion Chamber, High Temperature Materials, Heat Exchanger, Thermal Barrier Coating.

1 INTRODUCTION

High speed combustion chamber used in aero-space domain has to be designed to withstand the temperatures and thermo-structural stresses prevailing due to the thermal gradients and pressure forces. Without sufficient cooling no material can withstand such high temperatures. So, to cool the structure, active cooling, using the fuel as coolant, is seen as a viable option. In this process the fuel will be reformed due to pre-heated, which helps in better combustion. The preheating also has the advantage of augmenting heat sink capacity of the fuel due to endothermicity. The challenge in such active cooling system is availability of the fuel on board that can be used as coolant. Though the cooling efficiency is a function of geometric parameters and thermo-physical properties of materials, the manufacturing constraints and the material choices, keeps the fuel flow rate required about 3 times in excess of stoichiometric combustion requirements. Carrying excess fuel on board adds up to the weight penalty. In order to reduce the coolant flow rate, the use of Thermal Barrier Coatings (TBCs) has been pursued by many researchers. But there are wide variety of TBC coatings available based on the application. For the application to the liners of high speed combustion chamber, the TBC coatings must possess low thermal conductivity, high phase stability, the thermal expansion must match the metallic substrate, high melting point. Based on the above requirements Lanthanum Zirconium Oxide (La₂Zr₂O₇) [1], Lanthanum Cerium Oxide (La₂Ce₂O₇) [2], Yittria stabilized zirconia (YSZ) [2] were selected for investigation. Also, the coolant channel materials selected were Inconel X-750[3] [4], Nb-Cb752 [7] and GRCop-

84 [5], which have high temperature limits and high yield strength at elevated temperatures.

2 METHODOLOGY

The actively cooled combustor liner as shown in the Fig.1 has channels running along the length of the panel. The fuel used as coolant flows through these channels to absorb the heat flux impinging on the panel. In the current paper, comparative performance of the active cooling channel was studied for a combination of different coolant channel materials, TBC materials and channel cross sections. Table 1 and Table 2 provide the thermo-physical properties of the TBC materials and the metal alloys used for the investigation. Fig.2 shows the two channel cross sections used for the investigation. This study helps to identify the appropriate combination of the TBC material, coolant channel material and the shape suitable for the application. For the investigation, various researchers proposed different analytical models. Youn and Mills [6] proposed an analytical by considering 3 fins, the face (t_f) and two cores (t_c), with two corners for a single channel. Valdevit et al. [7] proposed an analytical model by considering cores (t_c) as fins considering critical points across the cross section, to calculate temperatures and stresses at these points. For the investigation, 1-D analytical model was developed by following the approach of Valdevit et al. [7] for rectangular cross section. For trapezoidal cross section the analytical model was derived and presented. MATLAB program was used for calculating the temperature and stresses experienced for the cooling channel. 2D thermo-structural analysis was carried out in ANSYS 14.5 to verify the 1-D calculation. MATLAB program was used subsequently to verify several rectangular and trapezoidal cross sections by varying geometric parameters based on the manufacturing feasible dimensions provided in Table 3. Finally the graphs were generated based for minimum weight per unit area for a given mass flow rate of coolant.

- Siva Karthik C V S S is a Research Scholar in Mechanical Engineering Department, Jawaharlal Nehru Technological University, Hyderabad, India. E-mail: seva.karthik@gmail.com
- Santhosh Kumar N, pursuing Masters in Thermal Engineering, Jawaharlal Nehru Technological University, Hyderabad, India.
- T. Kishen Kumar Reddy, Professor Mechanical Engineering Department, Jawaharlal Nehru Technological University, Hyderabad, India.

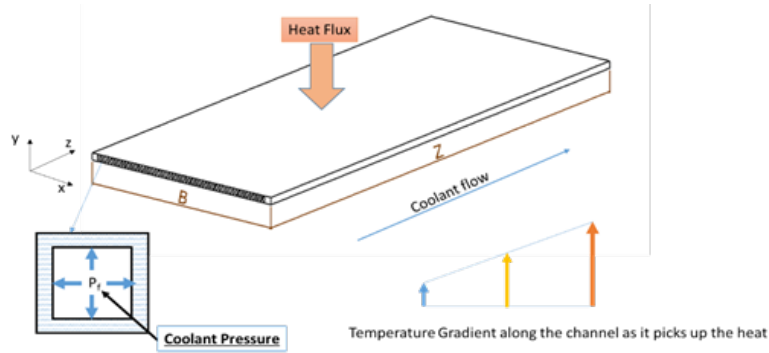


Fig.1. Active Cooling Panel

Table 1. TBC material properties

TBC Material	Thermal conductivity (W/m/K)	Density (Kg/m ³)	Thermal expansion coefficient (K ⁻¹)
YSZ	1	6000	5x10 ⁻⁶ to 11x10 ⁻⁶
La ₂ Zr ₂ O ₇	0.8	6050	6x10 ⁻⁶ to 10x10 ⁻⁶
La ₂ Ce ₂ O ₇	0.68	4644	10x10 ⁻⁶ to 13x10 ⁻⁶

Table 2. Material Properties

Material	Usage Temperature (K)	Density (Kg/m ³)	Coefficient of thermal expansion (10 ⁻⁶ / K)	Coefficient of thermal conductivity (W/m ² K)	Yield Stress (MPa)	$\frac{d\sigma}{dT}$ (MPa/K)	Young's Modulus (GPa)
GRCop-84	973	8756	19	285	205	-0.18	90
Nb-Cb752	1470	9030	7.4	50	382	-0.39	110
Inconel X-750	1100	8276	16	23	795	-0.17	128

Table 3. Range of geometric parameters

Sl.no	Geometric Parameter	Dimensions (m)
1	Channel width (w)	0.0015-0.0025
2	Channel Height (L)	0.005
3	Web thickness (t _w)	0.0015
4	Core thickness (t _c)	0.00125

In case of trapezoidal cross section t_{c1} is maintained such that t_c-t_{c1} = 0.0005 m

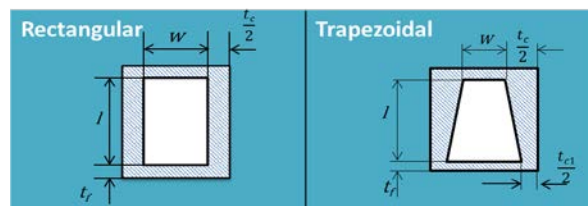


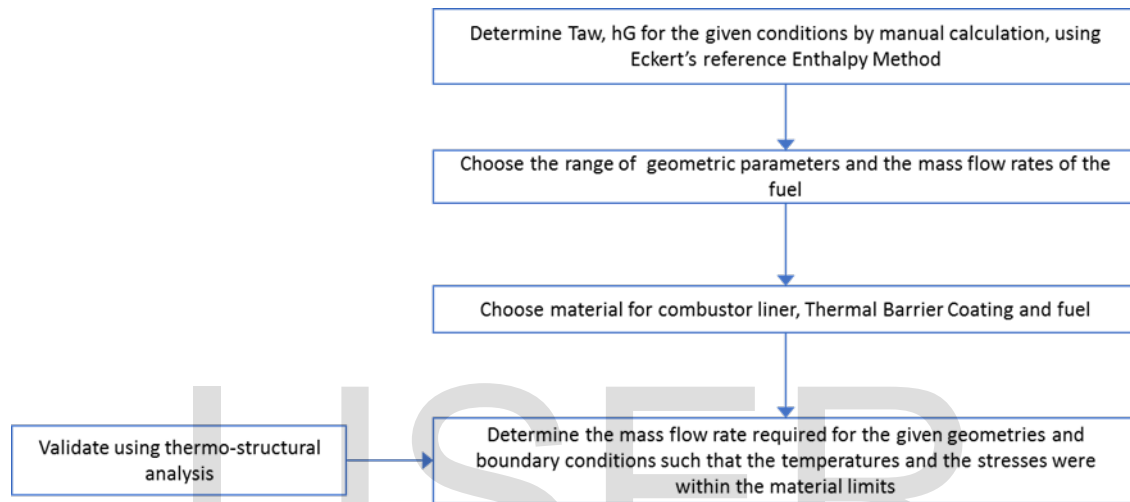
Fig.2 Different channel shapes used in the investigation

2.1 Analytical Model

Fig. 3 shows the flow chart for the MATLAB program used for making the calculation. For the rectangular channel the temperatures and stresses were calculated at the 18 critical points as shown in Fig.4. For the trapezoidal channel they have been derived and are shown in the following sections.

Temperature model: The temperatures along the channel were calculated based on the thermal resistance network shown in Fig.5. In order to incorporate the different shapes of the channel in to the program, following changes were made to the original program (a) Fuel mass flow rate per unit width, directly mass flow rate of the coolant per channel was provided

as an input. (b) The thermal resistances [7] of rectangular and trapezoidal fin shapes given in Table 4 were incorporated. The length of the channel was taken as 0.7 m. The inputs required are the realistic adiabatic wall temperature (T_{aw}), heat transfer coefficient on combustion side (hG), coolant mass flow rate (\dot{m}_f), inlet temperature of the coolant (T_f^0) as encountered in experimental test conditions. The hydrocarbon fuel JP-7 is used as a coolant throughout this investigation. The heat transfer coefficient (hG) was calculated as per the reference enthalpy method [8] [9].



Note: T_{aw} – Adiabatic Wall Temperature; hG – Heat Transfer coefficient on the side of combustion gases

Fig.3: Flow chart for the methodology followed

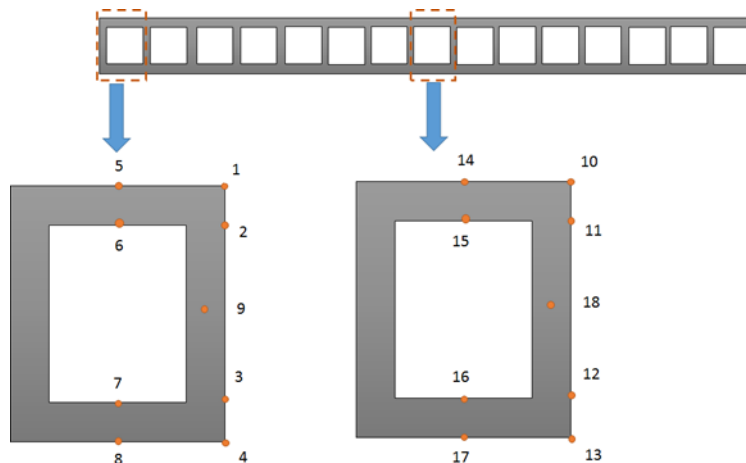
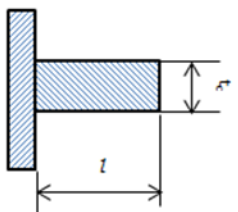
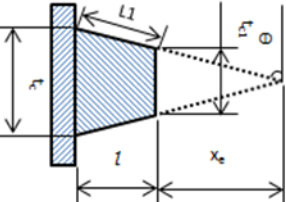


Fig.4. Critical points identified on the panel for evaluating the stresses and temperature

Table 4. Fin Resistances of different shapes

Fin Type	Resistance of Fin (R_{fin})	Area of fin (A_f)
<p>Rectangular fin</p> 	$R_{fin} = \frac{ml}{h_c A_f \tanh (ml)}$ $m = \left[\frac{2 h_c}{k t_c} \right]^{0.5}$	$A_f = 2 l t_c$
<p>Trapezoidal fin</p> 	$R_{fin} = \frac{ml}{h_c A_f} \frac{I_0(2ml)K_1(2m\sqrt{lx_e}) + K_0(2ml)I_1(2m\sqrt{lx_e})}{I_1(2ml)K_1(2m\sqrt{lx_e}) + K_0(2ml)I_1(2m\sqrt{lx_e})}$ $m = \left[\frac{2 h_c}{k t_c} \right]^{0.5}$	$A_f = [(t_c - t_{c1})l + 0.5 t_{c1}l]$

Temperatures for a Trapezoidal cross section:

The temperatures formulae at the 18 critical points for the rectangular channel were taken as per [6] and for the trapezoidal channel they differ from that of the rectangular channel only at the points 3, 4, 7, 8, 9, 12, 13, 16, 17 and 18 and are given as follows.

$$T^{(i)} = T_f + (T^{(2)} - T_f^0) \cdot \frac{I_0(2m\sqrt{lx_e}) K_1(2m\sqrt{lx_e}) + K_0(2m\sqrt{lx_e}) I_1(2m\sqrt{lx_e})}{I_0(2ml) K_1(2m\sqrt{lx_e}) + K_0(2ml) I_1(2m\sqrt{lx_e})} \text{ at points 3,4,7,8,12,13,16, and 17}$$

$$T^{(i)} = T_f + (T^{(2)} - T_f^0) \cdot \frac{I_0(2m\sqrt{l/2}) K_1(2m\sqrt{lx_e}) + K_0(2m\sqrt{l/2}) I_1(2m\sqrt{lx_e})}{I_0(2ml) K_1(2m\sqrt{lx_e}) + K_0(2ml) I_1(2m\sqrt{lx_e})} \text{ at points 9 and 18}$$

Where $m = (2 \cdot h_c / (k_{fin} \cdot t_c))^{0.5}$ ----- (B1)

Fuel temperature

The fuel temperature is obtained by the energy balance equation given below. The amount of the heat emery absorbed by the fuel is equal to amount of energy given by the channel material.

$$\frac{d(T_{aw} - T_f)}{dz} + \frac{1}{R_1 m_f c_{pf}} \left(\frac{w}{w + t_c} R_w^* + \frac{t_c}{w + t_c} R_c^* \right) (T_{aw} - T_f) = 0$$

$$m_f c_{pf} \frac{dT_f}{dz} = \frac{w q_w(z) + t_c q_c(z)}{w + t_c}$$

The solution for the above differential equation is

$$\frac{T_{aw} - T_f}{T_{aw} - T_f^0} = \exp(-\beta z) \text{ Where, } \beta = \frac{1}{R_1 m_f c_{pf}} \left(\frac{w}{w + t_c} R_w^* + \frac{t_c}{w + t_c} R_c^* \right) \text{ ----- (B2)}$$

2.2 Thermo-Structural stresses Model

To obtain analytical estimates of the stresses following assumptions are made

- Uniform thermal expansion is permitted in all directions.
- The combustion pressure does not cause panel-level bending.
- The coolant pressure P_f induces uniform tensile stresses in the core members.
- The temperature variation along the panel length has been neglected. This assumption, combined with the imposed boundary conditions, ensures that generalized plane strain conditions are attained along the z-direction.
- The stress due to the pressure of the combustion gases is ignored as the bottom of the channel is supported against bending and since the $P_{comb} \ll P_f$ the stresses are neglected. The load is taken by the face members and the stress on the core member can be neglected.

Based on these assumptions analytical expressions are derived for calculating stresses at 18 critical points of the channel.

Mechanical Analytical Model

For the trapezoidal cross-section, the mechanical stresses were derived as follows. Due to the coolant pressure tensile stresses are induced at points 9, 18.

$$\frac{\sigma_{core,y}^{P_f}}{P_f} = \frac{2w}{(t_c + t_{c1})}, \quad \frac{\sigma_{core,z}^{P_f}}{P_f} = \nu \frac{\sigma_{core,y}^{P_f}}{P_f}$$

$$\theta = \tan^{-1}(2l/(t_c - t_{c1}))$$

$$L1 = \sqrt{(L^2 + t_{c1}^2)}$$

$$\frac{\sigma_{face,x}^{P_f}}{P_f} = ((L1 \sin(\theta))/(2t_f) - (0.5 * (w/t_f)^2)) \quad \text{at points 1,10}$$

$$\frac{\sigma_{face,x}^{P_f}}{P_f} = ((L1 \sin(\theta))/(2t_f) + (0.5 * (w/t_f)^2)) \quad \text{at points 2, 11}$$

$$\frac{\sigma_{face,x}^{P_f}}{P_f} = ((L1 \sin(\theta))/(2t_f) - (0.25 * (w/t_f)^2)) \quad \text{at points 6, 15}$$

$$\frac{\sigma_{face,x}^{P_f}}{P_f} = ((L1 \sin(\theta))/(2t_f) + (0.25 * (w/t_f)^2)) \quad \text{at points 5, 14}$$

$$\frac{\sigma_{face,x}^{P_f}}{P_f} = ((L1 \sin(\theta))/(2t_f)) \quad \text{at points 3, 12}$$

$$\frac{\sigma_{face,x}^{P_f}}{P_f} = ((L1 \sin(\theta))/(2t_f)) \quad \text{at points 4, 13}$$

$$\frac{\sigma_{face,x}^{P_f}}{P_f} = ((L \sin(\theta))/(2t_f)) \quad \text{at points 7, 16}$$

$$\frac{\sigma_{face,x}^{P_f}}{P_f} = ((L1 \sin(\theta))/(2t_f)) \quad \text{at points 8, 17}$$

----- (B3)

Thermal Stresses

The temperature difference across the top face causes compression along its top surface and tension along its bottom surface (at the boundary with the coolant). These stresses are:

$$\sigma_{face,z}^{\Delta T_{tf}} = \sigma_{face,z}^{\Delta T_{tf}} = -\frac{E\alpha\Delta T_{tf}}{2(1-\nu)} \quad \text{at points 1, 5, 10, and 14}$$

$$\sigma_{face,x}^{\Delta T_{tf}} = \sigma_{face,z}^{\Delta T_{tf}} = \frac{E\alpha\Delta T_{tf}}{2(1-\nu)} \quad \text{at points 2, 6, 11, and 15}$$

----- (B4)

With E and α the Young modulus and the coefficient of thermal expansion of the material, respectively. Additionally, the average temperature difference between the top and bottom faces,

$$\Delta T_{panel} = (\Delta T_{panel}^w + \Delta T_{panel}^c)/2 \quad \text{----- (B5)}$$

causes the panel to deform uniformly in each of the x- and z-directions, inducing compression in the top face and tension in the bottom face. Accounting for the stretching stiffness of the core members along the z-direction and assuming that the temperatures of the core and the bottom face are the same at steady state, the resulting additional stresses are

$$\sigma_{face,z}^{\Delta T_{panel}} = -\frac{E\alpha\Delta T_{panel}(A_f + A_c)}{2(1-\nu)(2A_f + A_c)} \quad \text{at Points 1, 2, 5, 6, 10, 11, 14, and 15}$$

$$\sigma_{face,z}^{\Delta T_{panel}} = \frac{E\alpha\Delta T_{panel}A_f}{2(1-\nu)(2A_f + A_c)} \quad \text{at Points 3, 4, 7, 8, 12, 13, 16, and 17}$$

----- (B6)

Where $A_f = t_f(w + t_c)$ and $A_c = t_c(H - 2t_f)$ are the cross-sectional areas of the face and the core in a unit cell, respectively. For both rectangular and trapezoidal cross sections, the B4 and B5 are applicable to calculate the thermal stresses.

2.4 Failure Criteria

For metals, failure is defined by the onset of yielding. The Von-Mises stress criterion is used which is

Max.

$$i=1-18 \left\{ \left(\frac{\sigma_{m,x}^{(i)}}{\sigma_Y(T^{(i)})} + \frac{\sigma_{T,x}^{(i)}}{\sigma_Y(T^{(i)})} - \frac{\sigma_{m,z}^{(i)}}{\sigma_Y(T^{(i)})} - \frac{\sigma_{T,z}^{(i)}}{\sigma_Y(T^{(i)})} \right)^2 + \left(\frac{\sigma_{m,x}^{(i)}}{\sigma_Y(T^{(i)})} + \frac{\sigma_{T,x}^{(i)}}{\sigma_Y(T^{(i)})} \right)^2 + \left(\frac{\sigma_{m,z}^{(i)}}{\sigma_Y(T^{(i)})} + \frac{\sigma_{T,z}^{(i)}}{\sigma_Y(T^{(i)})} \right)^2 \right\} = 2$$

With the stress components and the temperatures at each location 'i' given by equations B1 B2 B3 B4, B5, B6 respectively. The above criterion is applicable for both rectangular and trapezoidal cross sections.

3 ANALYTICAL VS NUMERICAL MODEL

In order to verify the results from the analytical model above, 2D thermo-structural analysis is carried out in ANSYS 14.5. Fig.6 provides the steps followed for the thermo-structural analysis. The analysis was carried out for both rectangular and trapezoidal configurations. The simulations are carried out for Nb-Cb752 material.

Boundary Conditions:

- Mechanical:

- Pressure on the channel wall - 3 MPa

- Thermal:

- Heat Transfer coefficient on the coolant side (derived from the Gnielinski Correlation)
- Temperature of the coolant (derived from the energy balance equation B2)
- Heat Transfer coefficient on the combustion side of the wall (derived from Eckert's Enthalpy condition) 697.5 W/m²K
- Adiabatic wall temperature 3297 K

- Supports:

The bottom portion is assumed to be on a bed rollers permitting expansion in all the directions. The panel level bending is restricted.

- The bottom wall is constrained against the movement in Y - Direction
- The left side wall is constrained against the movement in X - Direction
- In order to allow for the thermal expansion, the right side wall is allowed to displace uniformly in X - Direction

- Channel Material - Nb-Cb752

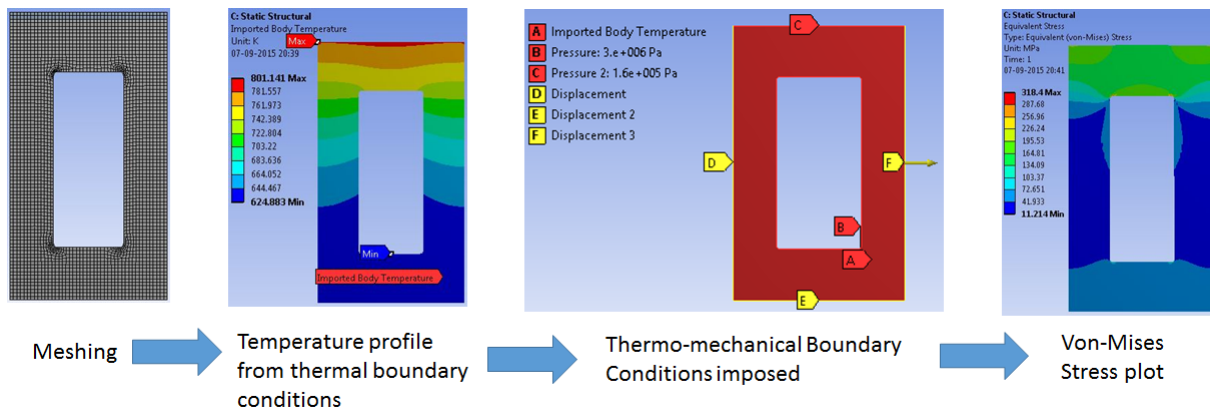


Fig.6. Thermo-structural analysis for rectangular channel

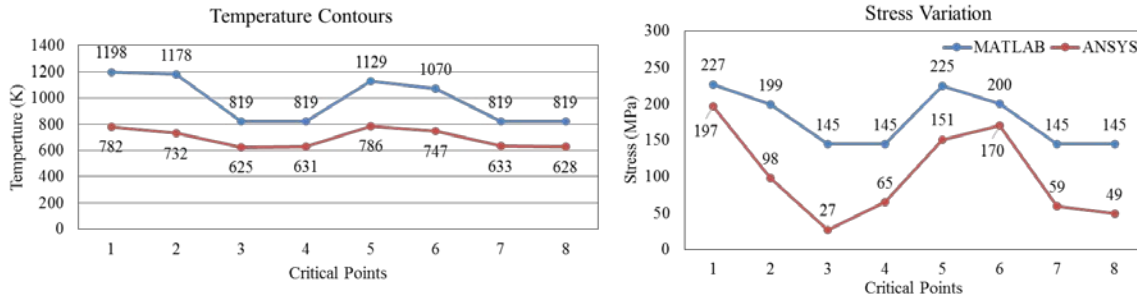


Fig.7. MATLAB and ANSYS Temperature and Stress results comparison at the critical points along the profile of the rectangular channel

The graphs in Fig.7 show the variation of temperatures and stresses for the rectangular channel configuration. It was observed that the temperatures obtained from the numerical model were 40% lower than the analytical model at the high temperature points. This could be mainly due to the 1-Dimensional formulation of the analytical model differing with that of the 2-Dimensional numerical model. Suryanarayana [11], reported a difference of 80% between 1-Dimensional and 2-Dimensional heat transfer rates. Hence the variation is within the acceptable range.

Also, the stresses from the numerical model are lower than predicted. This could be due to the lower temperatures in the numerical model resulting in lower stresses and the underlying assumptions of the analytical model. Hence the variations were within the predictable range. The trend observed for both temperatures and stresses was similar between MATLAB and Analytical results. Therefore the analytical model was used for further investigation over a range of geometric and material parameters. Similar trends were observed for the trapezoidal channel as well for both temperatures and stresses.

2.5 MATLAB Results

Using the MATLAB program, the results are obtained for a range of geometric parameters as listed below in Table 5. The thickness of the TBC considered was varied between 0.0001 to 0.0005 m. Analytical results using MATLAB program are obtained for the inlet temperature of the coolant (T_f^0) of 300 K, heat transfer coefficient on the combustion side (hG), 697.5 W/m²/K, adiabatic wall temperature (Taw) 3297 K and the length of the channel 0.7 m. The width of the panel 'B' was considered as 0.772 as shown in Fig.1. The coolant flow rate is varied between 0.001 Kg/s to 0.006 Kg/s. The graphs in Fig.8 show the minimum metal weight per unit area (metal weight alone) and minimum overall weight per unit area (metal and fuel consumed for a given flow time) against a given coolant flow rate. Here, the width of the panel is chosen a 0.772 m. The flow time considered for the calculation of the fuel weight is 30 seconds.

3 RESULTS AND DISCUSSION

Effect of TBC: From the above results it can be observed that the TBC helps to reduce the coolant mass flow rate required.

- For the material Inconel X-750, without TBC the minimum amount of coolant flow rate required was 0.0045 Kg/s for a single channel, whereas the coolant flow rate was 0.0015 Kg/s with TBC.

- Without TBC the minimum overall weight per unit for panel for the starting configuration was found to be 150 Kg/m² whereas the minimum overall weight with TBC was found to be 70 Kg/m² due to decrease in the amount of coolant flow rate for a given width of the panel.

- For all the combinations with TBC, both Inconel X-750 and Nb-Cb752 did not show any appreciable difference in terms of weight per unit area, whereas for GRCo-84 in combination with Lanthanum Cerium Oxide (La₂Ce₂O₇) has the lowest weight per unit area followed by Lanthanum Zirconium Oxide (La₂Zr₂O₇), and Yttria stabilized zirconia (YSZ). This is probably due to the lowest thermal conductivity of Lanthanum Cerium Oxide (La₂Ce₂O₇). Both Inconel X-750 and Nb-Cb752 were observed to have lowest weight per unit area in combination with TBC than without TBC. GRCo-84 was not able to withstand the thermo-structural stresses without TBC.

- Also, the combination of GRCo-84 with YSZ requires higher coolant flow rate among all the combinations investigated.

Effect of Channel Material:

- Among of channel materials considered, Inconel X-750 and Nb-Cb752 were found to have lower weight per unit area compared to the GRCo-84.

- Also, for GRCo-84 the minimum coolant flow rate required for an acceptable configuration was found to be 0.0035 Kg/s, which is higher than coolant channel flow rate for other two materials.

- At lower coolant flow rate the weight per unit area (metal weight alone) is high. This could be due to the thicker cross sections required to counter the higher thermal gradient at lower coolant flow rates.

- In case of Inconel X-750 and Nb-Cb752, the overall weight per unit area (metal and fuel) first decreases and then increases monotonically, whereas for GRCop-48, the trend showed very minimum variation compared to other two materials.

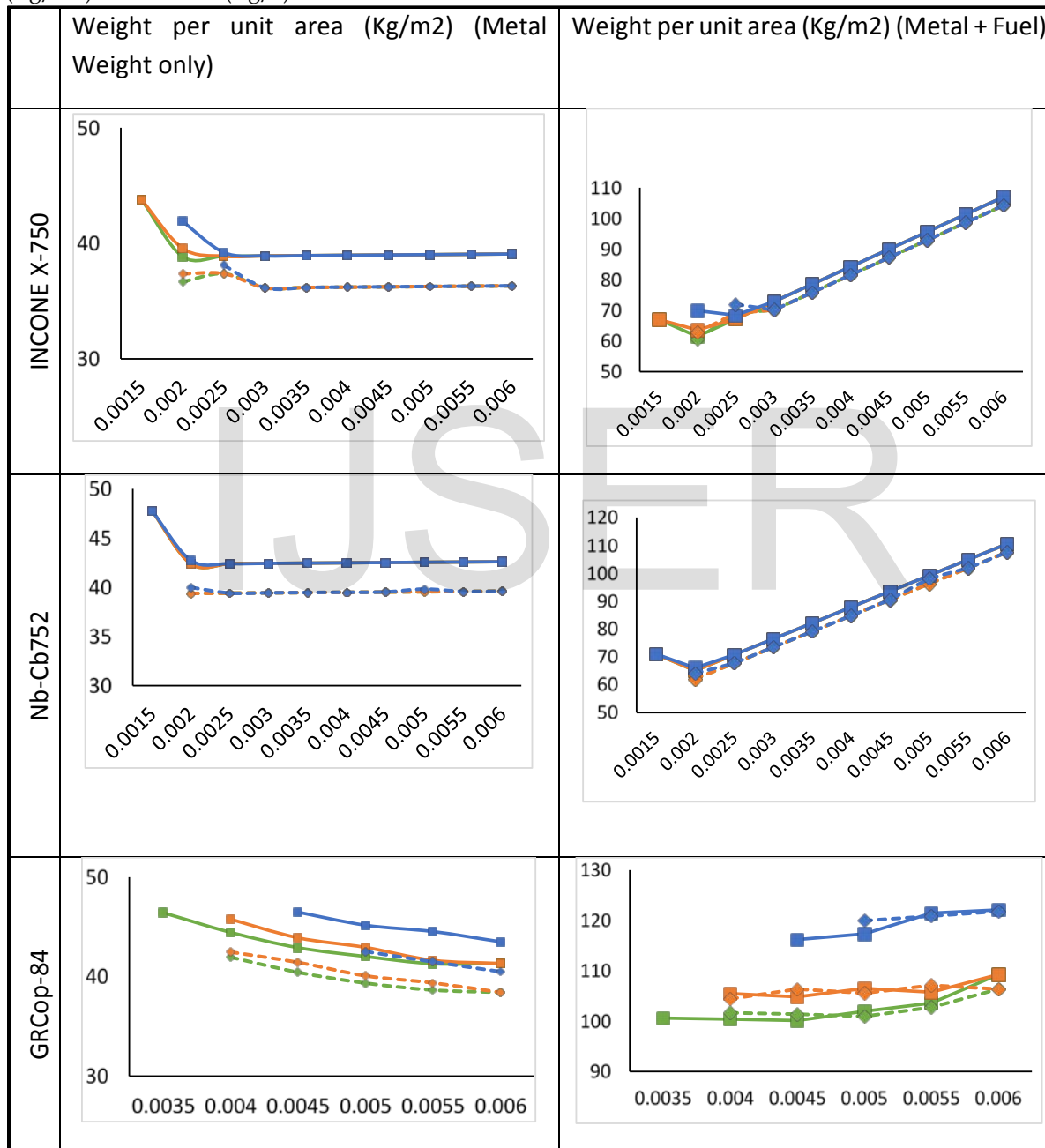
Effect of shape of the channel:

- The trapezoidal cross section, when compared to the

rectangular cross section was observed to have lowest weight per unit area but in terms of overall weight per unit area, no appreciable difference was observed.

- In all the combinations investigated, minimum coolant required for the trapezoidal was slightly higher than the rectangular ones.

Table 5. Graphs showing the minimum weight per unit area (Kg/m²) and overall weight per unit area (Kg/m²) Vs flow rate (Kg/s)



Legend:

- La₂Ce₂O₇ - Rectangular - - ■ La₂Ce₂O₇ - Trapezoidal
- La₂Zr₂O₇ - Rectangular - - ■ La₂Zr₂O₇ - Trapezoidal
- YSZ - Rectangular - - ■ YSZ - Trapezoidal

4 CONCLUSION:

- The analytical model was established for checking the feasibility of rectangular and trapezoidal cross sections.
- TBC has the effect of decreasing the coolant flow rate and reduced the weight per unit area. In case of Inconel X-750, the minimum coolant flow rate was 66% lower for the channel with TBC than for the channel without TBC.
- GRCo-84 was found to be viable only in combination with TBC only.
- In terms of weight per unit area, trapezoidal was found to be slightly lower than the rectangular channel for a given mass flow rate.
- In terms of overall weight per unit area, the starting configuration with TBC was found to be 50% lower than the configuration without TBC.

5 REFERENCES

1. X. Cao, R. Vassen, W. Fischer, F. Tietz, W. Jungen, D. Stover "Lanthanum Cerium Oxide as Thermal Barrier Coating Material for High Temperature Applications", *Advanced Materials* Vol.15-17, pp. 1438, September 2003.
2. Robert Vassen, Xueqiang Cao, Frank Tietz, Debabrata Basu, and Detlev Stöver, "Zirconates as New Materials for Thermal Barrier Coatings" *J. Am. Ceram. Soc.*, 83 [8] 2023–28 (2000)
3. www.specialmetals.com INCONEL® alloy X-750 (UNS N07750/W. Nr. 2.4669)
4. Tresa M. Pollock, Sammy Tin "Nickel-Based Superalloys for Advanced Turbine Engines: Chemistry, Microstructure, and Properties," *Journal of propulsion and power*, (22) No. 2, pp. 361-374, 2006.
5. David L. Ellis (2005) "GRCo-84: A High-Temperature Copper Alloy for High-Heat-Flux Applications", NASA/TM—2005-213566.
6. B. Youn and A. F. Mills, "Cooling Panel Optimization for the Active Cooling System of a Hypersonic Aircraft," *Journal of thermophysics and heat transfer* Vol. 9, No. 1, 1995
7. Lorenzo Valdevit, Natasha Vermaak, Frank W. Zok, Anthony G. Evans, "A Materials Selection Protocol for Lightweight Actively Cooled Panels", *Journal of Applied Mechanics* Copyright © 2008 by ASME NOVEMBER 2008, Vol. 75 / 061022-1
8. Frank P. Incropera, David P DeWitt, "Heat and Mass Transfer", Fifth edition, John Wiley & Sons, Inc., pp.141
9. Robert D. Quinn and Leslie Gong, "Real time aerodynamic heating and surface temperature calculation for hypersonic flight simulations," NASA technical memorandum, 4222, 1990.
10. Michael E. Tauber, "A Review of High-Speed, Convective, Heat-Transfer Computation Methods", NASA Technical Paper, 2914, 1984.
11. N.V.Suryanarayana, "Two dimensional effects on heat transfer rates from an array of straight fins", *ASME J. Heat Transfer* 99 (1977), pp. 129-132

NOMENCLATURE

h_G – Heat Transfer coefficient of the hot gases
 h_C – Heat Transfer Coefficient of the coolant inside the channel
 k_s – Thermal Conductivity of the metal
 k_f – Thermal Conductivity of the fuel / coolant
 w – width of the channel
 t_c – core thickness
 t_f – face thickness
 l – height of the channel
 A_f – Area of the face
 A_c – Area of the core
 L_1 – Angular length of the trapezoidal fin
 Θ – Angle
 t_{c1} – Thickness of the trapezoidal fin at the tip
 x_e – distance of the tip of the fin from origin
 I_0 – Bessel function of first kind and first order
 I_1 – Bessel function of first kind and second order
 K_0 – Bessel function of second kind and first order
 K_1 – Bessel function of second kind and second order
 Nu – Nusselt Number
 D_h – Hydraulic Diameter
 A – Flow area of the channel
 P – Flow perimeter of the channel
 f – friction factor
 Pr – Prandtl number
 u – flow velocity
 ν_f – Coolant dynamic viscosity
 b – width of the channel
 B – width of the panel
 W – Weight
 t – time in seconds
 N – Number of channels
 P – Pressure
 T – Temperature
 q – heat flux W/m^2
 m_f – mass of the fuel
 c_{pf} – Specific heat of the fuel
 E – Young's Modulus
 α – Thermal coefficient of expansion
 ν – Poisson ration
 P_{comb} – Combustion gas pressure
 ΔT_{panel} – Temperature gradient across the wall
 ΔT_{panel}^w – Temperature gradient across the web of the panel
 ΔT_{panel}^c – Temperature gradient across the core of the panel
 ΔT_{tf} – Temperature gradient across the tope face
 σ – Stress

Subscript
 P – Panel
 T – Thermal
 m – Mechanical
 aw – adiabatic wall temperature
 $fuel$ – fuel
 w – Web
 c – Core
 tf – mid of top face
 Y – Yield
 h – Combustion gases
 f – Fuel